

# *syn*-Sesquinorbornenyl carbocations and their boron analogues: an *ab initio* and DFT study † ‡

2 PERKIN

Mirjana Eckert-Maksić,\* Ivana Antol, Davor Margetić and Zoran Glasovac

Division of Organic Chemistry and Biochemistry, Rudjer Bošković Institute, P.O.B. 180, HR-10002, Zagreb, Croatia. E-mail: mmaksić@emma.irb.hr; Fax: +385 1 4680 195; Tel: +385 1 4680 197

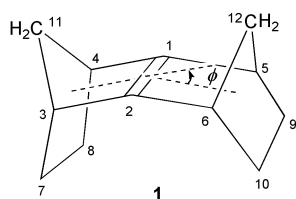
Received (in Cambridge, UK) 2nd August 2002, Accepted 7th October 2002

First published as an Advance Article on the web 25th October 2002

MP2 and DFT calculations employing 6-31G\* were carried out to investigate the structure of some of the carbocations and their boron analogues embedded in the *syn*-sesquinorbornene framework, hitherto not observed experimentally. The calculated minimum energy structures of all species provide evidence for homoconjugative interaction between the electron deficient center(s) and the carbon–carbon double bond. The use of isodesmic reactions based upon MP2(fc)/6-31G\* energies indicates that the homoconjugative stabilisation of mono- and dications is greater than those of the isoelectronic boron compounds. The calculated <sup>13</sup>C and <sup>11</sup>B NMR chemical shifts support this conclusion.

## Introduction

*syn*-Sesquinorbornene<sup>1</sup> **1** (Scheme 1) has intrigued chemists<sup>2–4</sup>



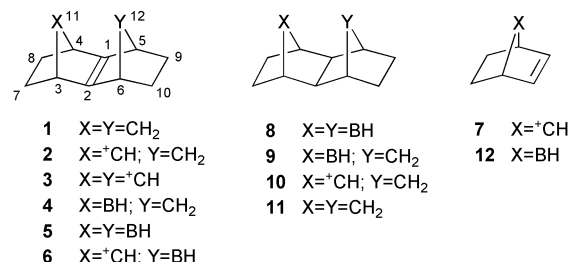
Scheme 1

since it was first prepared in the early eighties.<sup>5</sup> In the intervening years various aspects of the physico-chemical properties of the parent molecule and a number of its derivatives have been analysed, with particular emphasis on the pyramidalization of the olefinic carbon atoms and its consequence on reactivity. A number of X-ray studies of crystalline *syn*-sesquinorbornene derivatives also appeared in the meantime,<sup>6</sup> which have shown that the double bond in **1** indeed deviates from planarity, exhibiting hinge-like *endo* bending characterised by the out of plane angle  $\phi$ .<sup>7–11</sup> Closely related to this feature is an observation that such molecules exhibit pronounced  $\pi$ -facial selectivity in their addition reactions.<sup>6a</sup>

In recent years we have been concerned with the syntheses,<sup>12</sup> the spatial structure analyses<sup>13</sup> and the electronic structure investigations<sup>14</sup> of a variety of heteroatom analogues of **1**. Pursuing our interest in this field we present here results of the molecular orbital *ab initio* and DFT calculations for *syn*-sesquinorbornenyl carbocations and their isoelectronic boron analogous **2–6** shown in Scheme 2. Despite the fact that there are no experimental data for these species, they are interesting from a theoretical viewpoint because of their unique framework, which permits competition between two spatially remote electron deficient centers joined by a common, highly non-planar, double bond.

† Electronic supplementary information (ESI) available: key structural parameters of compounds **2–6**. See: <http://www.rsc.org/suppdata/p2/b2/b207552k/>.

‡ Dedicated to Professor D. E. Sunko on the occasion of his 80th birthday.



Scheme 2

In the present work, we will address the following questions, each of which is related to this issue. (1) Do the species under investigation exhibit homoaromatic 3-center/2-electron bonding?<sup>15</sup> (2) Is the interaction between the electron deficient center(s) and the central double bond, if present, stronger in carbocations or in their isoelectronic neutral boron analogues? (3) Which of the two electron deficient bridges, <sup>+</sup>CH or BH, influences molecular architecture of the *syn*-sesquinorbornene framework more strongly? (4) Do 3-center/2-electron or 4-center/2-electron bonding patterns take place in species involving two electron deficient centers adjacent to the central double bond? To put it in another way, do they correspond to minima on the potential energy surface?

## Computational methods

Various forms of molecules **2–6** have been optimised at the MP2 level,<sup>16</sup> as well as with the density functional Becke-3LYP method,<sup>17</sup> in conjunction with the 6-31G\* basis set,<sup>18</sup> within the symmetry constraints specified in Tables 1 and 2. The nature of each stationary point was investigated by a full vibrational analysis at the same theoretical level used in the geometry optimisation. Vibrational zero-point energy corrections were applied using the scaling factors: 0.9670 and 0.9806 for the MP2 and B3LYP calculations, respectively.<sup>19</sup> In exploring the minimum energy paths for isomerization reactions involving location of the transition structures, the concept of the intrinsic reaction coordinate (IRC)<sup>20</sup> has been utilised within the framework of the B3LYP/6-31G\* theory.

**Table 1** Key structural parameters of cations **2** and **3** calculated at the MP2/6-31G\* level of theory<sup>a</sup>

Bond or angle	Cation				
	2a (C <sub>s</sub> )	2b (C <sub>s</sub> )	3a (C <sub>2v</sub> )	3b (C <sub>2v</sub> )	3c (C <sub>s</sub> )
C(1)–C(2)	1.419	1.372	1.443	1.374	1.423
C(2)–C(3)	1.472	1.475	1.509	1.481	1.475
C(3)–C(7)	1.532	1.673	1.550	1.667	1.534
C(7)–C(8)	1.544	1.564	1.550	1.569	1.544
C(3)–X(11)	1.528	1.449	1.492	1.451	1.534
C(1)–X(11)	1.718	2.301	1.929	2.293	1.724
C(7)–X(11)	2.472	1.969	2.426	1.981	2.476
C(2)–C(6)	1.503	1.502	1.509	1.481	1.496
C(6)–C(10)	1.561	1.562	1.550	1.667	1.643
C(9)–C(10)	1.555	1.552	1.550	1.569	1.582
C(6)–Y(12)	1.544	1.548	1.492	1.451	1.643
C(1)–Y(12)	2.352	2.310	1.929	2.293	2.324
C(9)–Y(12)	2.390	2.381	2.426	1.981	2.006
X(11)···Y(12)	3.056	4.354	2.780	4.355	3.224
C(1)–C(2)–C(3)	109.3	109.4	108.0	109.5	109.4
C(2)–C(3)–C(7)	117.3	108.0	109.5	108.6	117.2
C(2)–C(3)–X(11)	69.8	103.8	80.0	102.9	69.9
C(3)–X(11)–C(4)	103.1	108.4	105.4	109.0	103.0
C(1)–C(2)–C(6)	106.8	107.7	108.0	109.5	108.3
C(2)–C(6)–C(10)	102.5	106.6	109.5	108.6	104.9
C(2)–C(6)–Y(12)	101.0	98.5	80.0	102.9	104.2
C(6)–Y(12)–C(5)	95.5	95.2	105.4	109.0	109.2
$\alpha$	81.6	157.1	97.2	154.6	81.8
$\alpha_1$	129.0	125.4	97.2	154.6	155.7
$\beta$	151.0	88.0	145.8	89.5	150.8
$\beta_1$	123.2	121.9	145.8	89.5	93.1
$\phi$	–16.6	14.3	–17.9	8.1	–18.2

<sup>a</sup> All distances are in Å and angles in deg; the numbering scheme is shown in Scheme 1.

The <sup>13</sup>C NMR and <sup>11</sup>B NMR chemical shifts were computed by the GIAO/B3LYP/6-311+G\*\* method<sup>21</sup> employing MP2 and B3LYP geometries. The <sup>13</sup>C chemical shifts are referenced relative to TMS. The <sup>11</sup>B chemical shifts were computed using B<sub>2</sub>H<sub>6</sub> as a gauge molecule and then scaled to BF<sub>3</sub>–Et<sub>2</sub>O [ $\delta$ (B<sub>2</sub>H<sub>6</sub>) = 16.6 vs. BF<sub>3</sub>–Et<sub>2</sub>O]. Atomic charges were obtained by using the mixed electron density partitioning based on the symmetric Löwdin orthogonalization procedure<sup>22</sup> and CHELPG atomic charges, which are designed to reproduce the molecular electrostatic potentials in the atomic monopole approximation.<sup>23</sup> Although atomic charges do not have rigorous physical meaning,<sup>24</sup> they have proved extremely useful in qualitative discussion of a number of molecular properties.<sup>25</sup>

All calculations were carried out with the GAUSSIAN 94<sup>26</sup> or GAMESS-US<sup>27</sup> programs implemented on Linux-based Pentium III PCs or a cluster of Pentium III and Athlon MP PCs at the Rudjer Bošković Institute.

## Results and discussion

We commence discussion with some general observations. Both B3LYP/6-31G\* (hereafter B3LYP) and MP2/6-31G\* (hereafter MP2) utilised here provide a reliable description of the geometry of pyramidalized olefins as shown earlier by us<sup>12,13</sup> and by others.<sup>28</sup> They have also been frequently used in studying homoaromatic species in spite of their well known tendency to overestimate the stability of non-classical structures.<sup>29</sup> However, since all of the species considered here are expected to exhibit the homoaromatic characteristics, their relative stabilities are expected to be well reproduced due to cancellation of errors. The calculated total energies and the vibrational zero-point energies at each of the theoretical levels are listed in Table 3, together with the characters of the stationary structures. The total and relative energies are corrected for the ZPE energies. The key bond lengths and angles of the optimised geometries

**Table 2** Key structural parameters of boron compounds **4**, **5** and **6** calculated at the MP2/6-31G\* level of theory<sup>a</sup>

Bond or angle	Boron compound				
	4 (C <sub>s</sub> )	5 (C <sub>2v</sub> )	6a (C <sub>s</sub> )	6b (C <sub>s</sub> )	6c (C <sub>s</sub> )
C(1)–C(2)	1.406	1.423	1.436	1.426	1.416
C(2)–C(3)	1.462	1.491	1.485	1.475	1.494
C(3)–C(7)	1.536	1.544	1.536	1.532	1.639
C(7)–C(8)	1.545	1.550	1.546	1.544	1.581
C(3)–X(11)	1.631	1.599	1.511	1.525	1.447
C(1)–X(11)	1.765	1.974	1.801	1.723	2.326
C(7)–X(11)	2.569	2.521	2.451	2.471	2.003
C(2)–C(6)	1.511	1.491	1.494	1.490	1.458
C(6)–C(10)	1.556	1.544	1.558	1.586	1.536
C(9)–C(10)	1.557	1.550	1.551	1.565	1.544
C(6)–Y(12)	1.542	1.599	1.601	1.589	1.641
C(1)–Y(12)	2.353	1.974	2.160	2.410	1.758
C(9)–Y(12)	2.382	2.521	2.486	2.236	2.576
X(11)···Y(12)	3.131	2.774	2.795	3.172	3.252
C(1)–C(2)–C(3)	111.3	109.7	108.5	109.8	108.2
C(2)–C(3)–C(7)	115.5	110.2	115.1	117.5	105.8
C(2)–C(3)–X(11)	69.3	79.3	73.9	70.1	104.5
C(3)–X(11)–C(4)	98.2	98.9	103.8	103.1	108.5
C(1)–C(2)–C(6)	106.7	109.7	109.2	109.4	111.2
C(2)–C(6)–C(10)	104.5	110.2	105.7	103.6	115.7
C(2)–C(6)–Y(12)	100.8	79.3	88.4	103.0	69.3
C(6)–Y(12)–C(5)	94.9	98.9	98.1	98.8	97.8
$\alpha$	82.6	96.7	87.3	81.7	155.2
$\alpha_1$	128.0	96.7	110.9	141.0	82.4
$\beta$	150.1	144.0	148.7	150.9	92.8
$\beta_1$	122.2	144.0	135.5	108.2	149.9
$\phi$	–10.5	–14.1	–19.0	–18.3	–14.4

<sup>a</sup> All distances are in Å and angles in deg; the numbering scheme is shown in Scheme 1.

of the carbocations **2** and **3** are compiled in Table 1, whereas Table 2 summarises structural data for the boron compounds **4**, **5** and **6**. Also included in Tables 1 and 2 are the relevant out-of-plane angles  $\phi$  and the tilting angles  $\alpha$  [defined as the angle between the planes C(3)–C(4)–C(2)–C(1) and C(3)–C(4)–X(11)] and  $\beta$  [defined as the angle between the planes C(3)–C(4)–C(7)–C(8) and C(3)–C(4)–X(11)].

Comparison of the MP2 and B3LYP optimised geometries reveals that there is a reasonably good agreement between the two sets of data, although in general the former approach yields systematically longer carbon–carbon double bonds than the DF theory.<sup>30</sup> The opposite holds for carbon–carbon single bonds. There is also a reasonably good agreement between the calculated geometries and the available X-ray data for structurally related solid state structures. All the structures discussed in the following refer to MP2 calculations, unless noted otherwise, because B3LYP results are similar and lead to the same conclusion. Geometries obtained at the B3LYP level are given in Supporting information (Tables S1 and S2)†. The calculated <sup>13</sup>C and <sup>11</sup>B NMR chemical shifts and charges are listed in Tables 4 and 5, respectively.

## Energies and geometries of *syn*-sesquinorbornenyl carbocations

Common to all carbocations examined in the present work is the presence of the norbornen-7-yl carbocation cage (**7**), which belongs to the most thoroughly studied positively charged reactive intermediates in organic chemistry.<sup>31</sup> Based on the high rate and overall retention of configuration observed in the solvolysis of *anti*-norbornen-7-yl toluene-*p*-sulfonate Winstein<sup>32a</sup> and Roberts<sup>32c</sup> proposed that ion **7** has a non-classical structure. This was further confirmed by examination of the parent ion under long lived conditions,<sup>33</sup> theoretical studies<sup>33,34</sup> and X-ray analysis of some of its crystalline salts.<sup>35</sup>

Insertion of **7** into the *syn*-sesquinorbornene framework leading to carbocation **2** does not influence the character of

**Table 3** Total energies, vibrational zero point energies and characterization of stationary points for the different species. Parameters are collected at the MP2/6-31G\* and B3LYP/6-31G\* levels.

Compound	MP2/6-31G*				B3LYP/6-31G*			
	$E_{\text{tot}}/\text{au}^a$	ZPE/au <sup>b</sup>	$E_{\text{rel}}/\text{kcal mol}^{-1}$	$N_{\text{Imag}}$	$E_{\text{tot}}/\text{au}^a$	ZPE/au <sup>b</sup>	$E_{\text{rel}}/\text{kcal mol}^{-1}$	$N_{\text{Imag}}$
<b>2a</b>	-464.17572	0.23898	0.0	0	-465.75752	0.23845	0.0	0
<b>2b</b>	-464.11228	0.23653	39.8	1	-465.70107	0.23629	35.4	1
<b>2c</b>	-464.16298	0.23718	8.0	0	-465.76384	0.23685	-4.0	0
<b>3a</b>	-463.11335	0.22435	0.0	0	-464.67581	0.22384	0.0	0
<b>3b</b>	-463.08449	0.22169	18.1	2	-464.65366	0.22165	13.9	2
<b>3c</b>	-463.11512	0.22351	-1.1	1	-464.67787	0.22319	-1.3	1
<b>4</b>	-451.20764	0.23492		0	-452.77816	0.23408		0
<b>5</b>	-437.38940	0.21845		0	-438.92684	0.21759		0
<b>6a</b>	-450.34720	0.22230	0.0	0	-451.89679	0.22164	0.4	0
<b>6b</b>	-450.34699	0.22209	0.1	0	-451.89741	0.22153	0.0	0
<b>6c</b>	-450.30336	0.22036	27.5	1	-451.85500	0.21974	26.6	1

<sup>a</sup> Corrected for ZPE. <sup>b</sup> Scaled by factor 0.9670 and 0.9806 for MP2 and B3LYP calculations, respectively.

**Table 4** Comparison of calculated <sup>13</sup>C- and <sup>11</sup>B-NMR chemical shifts for *syn*-sesquiorbornenyl cations and their boron analogues, as calculated by the GIAO/6-311+G\*\* method at the B3LYP and MP2 geometries, the latter being given within parentheses<sup>a</sup>

Compound	Atom						
	C(1)	C(3)	C(7)	X(11)	C(6)	C(10)	Y(12)
<b>2a</b>	149.1 (147.6)	61.9 (62.5)	31.5 (31.5)	28.2 (24.7)	47.9 (46.5)	27.8 (27.4)	54.6 (53.5)
<b>2b</b>	161.0 (164.3)	63.7 (60.0)	14.8 (9.6)	235.1 (213.1)	49.8 (48.7)	28.6 (28.0)	58.1 (58.5)
<b>3a</b>	142.5 (140.2)	61.2 (59.5)	29.5 (28.9)	131.1 (117.0)	61.2 (59.5)	29.5 (28.9)	131.1 (117.0)
<b>3b</b>	159.7 (161.7)	63.1 (59.9)	13.2 (8.8)	243.8 (225.5)	63.1 (59.9)	13.2 (8.8)	243.8 (225.5)
<b>4</b>	138.9 (138.3)	51.7 (52.9)	35.8 (36.1)	-74.9 (-92.1)	48.4 (47.2)	31.0 (30.9)	51.3 (50.5)
<b>5</b>	134.9 (134.4)	40.0 (39.2)	32.5 (32.6)	-44.1 (-62.9)	40.0 (39.2)	32.5 (32.6)	-44.1 (-62.9)
<b>6a</b>	147.6 (144.8)	55.1 (53.4)	30.3 (29.7)	33.2 (30.7)	41.5 (41.2)	27.7 (28.2)	21.4 (-7.3)
<b>6b</b>	150.6 (148.9)	61.0 (61.9)	31.5 (31.4)	36.7 (34.2)	42.2 (42.0)	19.2 (18.1)	49.0 (33.3)
<b>6c</b>	134.3 (132.9)	67.0 (63.4)	13.3 (8.7)	271.0 (252.1)	61.0 (63.4)	35.9 (36.1)	-66.3 (-85.2)
<b>7</b>	130.7 (129.7)	63.4 (64.4)	30.2 (30.2)	33.9 (26.6)			
<b>12</b>	122.8 (121.5)	53.4 (55.3)	34.7 (34.9)	-74.2 (-93.2)			

<sup>a</sup> For the numbering of atoms see Scheme 1.

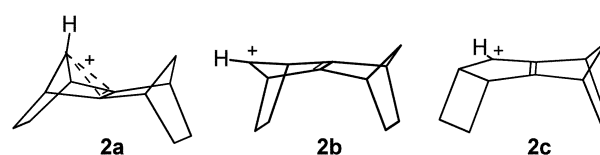
**Table 5** Löwdin's and CHELPG (in parentheses) formal charges of **2–6** as extracted from MP2/6-31G\* wavefunctions<sup>a</sup>

Atom	<b>2a</b>	<b>2b</b>	<b>3a</b>	<b>4</b>	<b>5</b>	<b>6a</b>	<b>6b</b>
C1	0.07 (0.13)	-0.03 (-0.04)	0.12 (0.09)	0.02 (0.13)	0.05 (0.17)	0.09 (0.11)	0.07 (0.17)
C3	-0.11 (-0.08)	-0.14 (-0.01)	-0.11 (-0.02)	-0.17 (-0.22)	-0.18 (-0.20)	-0.12 (-0.02)	-0.11 (-0.09)
C7	-0.29 (-0.02)	-0.25 (-0.04)	-0.28 (0.00)	-0.28 (0.01)	-0.28 (0.00)	-0.28 (0.00)	-0.29 (-0.03)
X11	-0.05 (0.00)	0.09 (0.11)	0.07 (0.18)	-0.28 (0.05)	-0.18 (0.17)	-0.03 (-0.02)	-0.05 (0.01)
C6	-0.14 (-0.03)	-0.14 (0.05)	-0.11 (-0.02)	-0.14 (-0.01)	-0.18 (-0.20)	-0.18 (-0.19)	-0.19 (-0.23)
C10	-0.29 (-0.06)	-0.30 (-0.01)	-0.28 (0.00)	-0.17 (-0.08)	-0.28 (0.00)	-0.28 (0.05)	-0.27 (-0.04)
Y12	-0.28 (-0.11)	-0.27 (-0.21)	0.07 (0.18)	-0.29 (-0.11)	-0.18 (0.17)	-0.05 (0.39)	-0.02 (0.35)
H3	0.21 (0.13)	0.22 (0.12)	0.24 (0.14)	0.17 (0.08)	0.17 (0.06)	0.21 (0.12)	0.21 (0.13)
H7 <i>exo</i> -	0.19 (0.07)	0.20 (0.09)	0.21 (0.10)	0.16 (0.02)	0.16 (0.03)	0.19 (0.06)	0.19 (0.08)
H7 <i>endo</i> -	0.19 (0.05)	0.22 (0.12)	0.22 (0.08)	0.15 (0.00)	0.15 (0.00)	0.19 (0.05)	0.19 (0.06)
H5	0.19 (0.07)	0.18 (0.05)	0.24 (0.14)	0.16 (0.03)	0.17 (0.06)	0.20 (0.08)	0.20 (0.10)
H9 <i>exo</i> -	0.19 (0.08)	0.18 (0.04)	0.21 (0.10)	0.16 (0.05)	0.16 (0.03)	0.19 (0.05)	0.19 (0.09)
H9 <i>endo</i> -	0.18 (0.05)	0.15 (0.00)	0.22 (0.08)	0.16 (0.02)	0.15 (0.00)	0.17 (0.01)	0.19 (0.06)
H11	0.23 (0.16)	0.23 (0.17)	0.25 (0.15)	0.08 (-0.12)	0.09 (-0.12)	0.24 (0.16)	0.23 (0.14)
H12 <i>syn</i> - <sup>b</sup>	0.17 (0.05)	0.17 (0.06)	0.25 (0.15)	0.17 (0.05)	0.09 (-0.12)	0.10 (-0.13)	0.11 (-0.09)
H12 <i>anti</i> -	0.18 (0.11)	0.17 (0.12)		0.15 (0.05)			

<sup>a</sup> For numbering of atoms see Scheme 1. The position of the hydrogen atoms is indicated by the number of the corresponding heavy atom given in italics. <sup>b</sup> With respect to the central double bond.

the ion to any great extent. Among two possible structural alternatives, **2a** and **2b**, only non-classical form **2a** is a minimum energy stationary point at both levels of theory.

Optimisation starting from the geometry with a hydrogen atom at the cationic center oriented opposite to the central double bond, and assuming that the system has a plane of



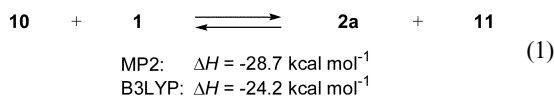
symmetry, gave rise to a structure **2b** with one imaginary frequency ( $\nu = 481\text{ i cm}^{-1}$ ) associated with the motion of the  $^+\text{CH}$  group out of the molecular symmetry plane. Reoptimisation of the latter structure without imposing symmetry constraints converged to a cation **2c**, which is more stable by  $31.8\text{ kcal mol}^{-1}$ .<sup>36</sup>

The geometry of the norbornen-7-yl part in **2a** is very similar to that computed for the parent cation. The C(11) carbon bridge leans toward the double bond with C(1)–C(11)/C(2)–C(11) distances ( $1.718\text{ \AA}$ ) much shorter than the C(7)–C(11)/C(8)–C(11) distances ( $2.472\text{ \AA}$ ). The former bond distances are very close to that calculated for norbornen-7-yl carbocation ( $1.723\text{ \AA}$ ) at the same level of theory,<sup>37</sup> and are in reasonable agreement with available X-ray data.<sup>35</sup> Concomitant with a disparity in C(1)–C(11) and C(7)–C(11) distances, there is also a pronounced difference in the tilting angles  $\alpha$  ( $81.6^\circ$ ) versus  $\beta$  ( $151.0^\circ$ ). The analogous angles in the structure of the norbornen-7-yl cation are  $81.4^\circ$  and  $150.5^\circ$ , respectively. In addition, there is a substantial increase in the double-bond distance ( $1.419\text{ \AA}$ ) of **2a** relative to **1** ( $1.361\text{ \AA}$ ), which may be compared with  $1.405\text{ \AA}$  and  $1.348\text{ \AA}$  in the norbornen-7-yl cation and norbornene, respectively.

Similarly, comparison of the calculated parameters for the neutral subunit in **2a** and **1** reveals that their geometries are also very close, apart the length of the double bond for reasons indicated above.

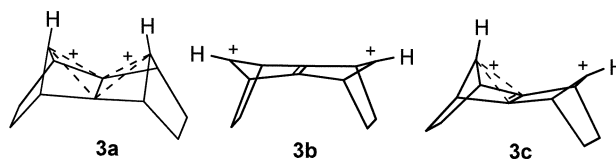
The most remarkable structural feature of **2a** pertinent to the present discussion is the occurrence of the *exo,exo*-bending of the molecular framework as evidenced by the out-of-plane angle  $\phi$  of  $-16.6^\circ$ , *i.e.* the opposite of that found in the neutral molecule ( $\phi = 16.4^\circ$ ). Not surprisingly, this is again in accordance with the out-of-plane angle of  $-23.0^\circ$  for the displacement of the olefinic hydrogen atoms in the norbornen-7-yl cation at the same level of theory (MP2). This finding clearly demonstrates that stabilisation gained by the 3-center/2-electron interaction in the norbornen-7-yl cage in **2a** is sufficient to enforce a change in direction of the out-of-plane bending relative to the neutral molecule. This is not surprising given that the bending potential for the central double bond in the sesquinorbornene skeleton is rather flat,<sup>28a</sup> as revealed by a frequency for the out-of-plane harmonic bending mode of  $139\text{ cm}^{-1}$  (MP2) in **2a**. The latter value is very close to the frequency of  $147\text{ cm}^{-1}$  in **1** calculated at the same level of theory.

In this regard it was of interest to estimate the stabilisation energy (SE) in **2a** due to interaction of the cationic center with the double bond. For this purpose we used the isodesmic reaction<sup>38</sup> shown in eqn. (1).

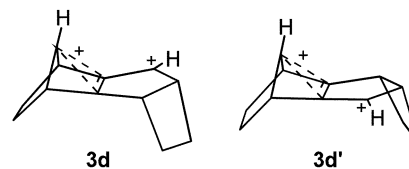


Both computational methods predict this reaction to be exothermic by  $-28.7\text{ kcal mol}^{-1}$  (MP2) and  $-24.2\text{ kcal mol}^{-1}$  (B3LYP), respectively, indicating significant stabilisation of **2a** due to interaction of the cationic center with the  $\pi$ -system of the double bond. This may be placed in perspective by comparison with the stabilisation energy of  $-25.9\text{ kcal mol}^{-1}$  in the norbornen-7-yl cation calculated by the MP2 method.<sup>32</sup>

We turn next to dication **3**, in which both of the  $\text{CH}_2$  bridges in **1** are replaced by the  $^+\text{CH}$  groups. It is reasonable to assume that the structure and stability of the resulting ion will be determined by an interplay of two opposing effects: (a) tendency of each of the charged centers to interact with the  $\pi$ -system of the double bond and (b) Coulombic repulsion of formal charges associated with the cationic centers. Among three possible structural alternatives, **3a–3c**, the form **3c** was found to have the lowest energy at both levels of theory employed.



Structure **3a**, with its two cationic centers oriented towards the double bond, thus permitting efficient overlap of “empty”  $2p_{\text{C}}$  orbitals with the  $\pi$ -bond charge cloud, was found to be  $\sim 1\text{ kcal mol}^{-1}$  less stable than **3c**. The structure **3b**, where the cationic centers are inclined toward ethano bridges, possess the highest energy (Table 3). Subsequent vibrational analysis, however, revealed that only the structure **3a** is the minimum energy stationary point on the Born–Oppenheimer potential energy surface. In contrast, it turned out that the structure **3c** is the transition structure ( $\nu = 350\text{ i cm}^{-1}$ ) for isomerisation of carbocation **3d** into **3d'** with an activation energy of  $4.4\text{ kcal mol}^{-1}$ . This conjecture was confirmed by subsequent IRC calculations.<sup>39,40</sup>



Similarly, two imaginary frequencies ( $412.2\text{ i}$  and  $413.8\text{ i cm}^{-1}$ ), each of them associated with displacement of the  $^+\text{CH}$  groups out of the symmetry plane passing through C(11) and C(12), were detected for the highest energy structure **3b**. It is interesting to note that energy barriers for isomerisation of **3d** into **3d'** is significantly higher than in the monocation series ( $31.8\text{ kcal mol}^{-1}$ ). Another point of interest is that dication **3d** (**3d'**) is found to be  $\sim 5.5\text{ kcal mol}^{-1}$  more stable than **3a** thus yielding thermodynamically the most stable isomer.

The most interesting form of dication **3** is its isomer **3a**, where the charged centers are located closest to each other. Its structural parameters clearly reveal that both cationic centers are inclined toward the central double-bond bridge, implying that they interact with the  $\pi$ -system of the double bond. In other words, the dication **3a** exhibits 4-center/2-electron bonding in contrast to **2a**. The resulting tilting angles ( $\alpha$  and  $\alpha'$ , respectively) and the related distances between the C(11) and C(12) atom(s) and the olefinic carbon atoms, are considerably larger than in **2a**, presumably due to charge–charge repulsion between the cationic centers. Evidently, the resulting separation of the C(11) and C(12) atoms ( $2.780\text{ \AA}$ , Table 1) represents a balance between the two opposing effects: (a) the charge–charge repulsion which tends to separate the charged centers as much as possible and (b) a tendency of the cationic centers to remain coplanar in order to maximise the overlap of the empty  $2p_{\text{C}}$ -orbitals with the doubly filled  $\pi$ -orbital of the C(1)–C(2) double bond.

As already mentioned earlier, the formal atomic charges do not have an absolute meaning. It is well known that Mulliken and atoms in molecule (AIM) charges are unrealistic, because they grossly exaggerate the intramolecular charge transfer.<sup>24</sup> More realistic in this respect are Löwdin charges,<sup>22</sup> which minimise the charge transfer. Additionally, we consider CHELPG atomic charges, which are designed to reproduce the molecular electrostatic potentials (MEP) as closely as possible, according to a certain prescription.<sup>23</sup> It is worth mentioning that atomic monopoles (charges) cannot satisfactorily describe MEPs. For that purpose a polycentric multipole expansion centered at each nucleus in a molecule is needed.<sup>24</sup> Hence, CHELPG atomic charges should be used with due caution. Keeping this in mind, we give atomic charges of the cationic carbon and the corresponding hydrogen atom attached to the

cationic center. They are 0.07 (0.18) and 0.25 (0.15) in  $|e|$ , respectively. One is tempted to conclude that Löwdin's partitioning somewhat underestimates the positive charge of the cationic centers. Nevertheless, both methods indicate that there is Coulombic repulsion between four positively charged atoms, which is in accordance with intuition.

Participation of the double bond in the homoaromatic interaction is evidenced by its length (1.443 Å), which is longer by 0.082 Å than in the neutral molecule **1** (1.361 Å). Another indicator is the pronounced pyramidalization of the olefinic carbon atoms in the *exo*-direction (*i.e.* the opposite of that in **1**). All these structural distortions lead to maximum overlap between a free p-orbital placed at each cationic center and the carbon-carbon double bond  $\pi$ -orbital, as mentioned above.

Comparison of the geometries of norbornen-7-yl cages in **3a** and **2a**, however, clearly shows that homoaromatic interaction is weaker in the former species. This conclusion is corroborated by comparing the charge distribution within the C(1)–C(11)–C(2) triangle in these two species (Table 5).

Finally, it is of interest to mention that the *anti*-conformer of **3a** is computed to be less stable than the *syn*-isomer by almost 8 kcal mol<sup>-1</sup> ( $E_{\text{tot}} = -463.32440$  au). The reason behind this seemingly counterintuitive result is simple. This is a 4-center/2-electron situation implying that there is only one molecular orbital occupied by two electrons. In the *syn*-case all four atomic orbitals overlap in-phase meaning that the resulting MO is strongly stabilised. In contrast, there is a node at carbon atoms forming a double bond in the *anti*-isomer in the corresponding 4-center molecular orbital. Consequently its orbital energy is raised leading to the lesser stability of this system.

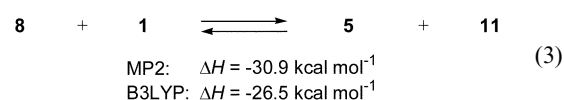
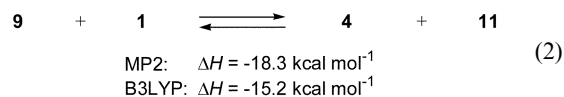
#### Geometries and energies of *syn*-borasesquinorbornenes

A strong structural resemblance between norbornen-7-yl carbocation (**7**) and 7-boranorbornene (**12**) had been predicted earlier by quantum chemical calculations<sup>38</sup> and was experimentally vindicated by X-ray crystal structure analysis of the Diels–Alder dimer of 1-phenyl-2,3,4,5-tetramethylborole.<sup>41</sup> Like norbornen-7-yl cation, its isoelectronic boron analogue (**12**), exhibits considerable homoaromatic interaction between the boron atom and the  $\pi$ -system of the olefinic double bond. The results in Table 2 provide firm support for the non-classical nature of the 7-boranorbornenyl cage in the boron analogues of *syn*-sesquinorbornenes **4** and **5**. This is evidenced by characteristic bending of the BH bridges toward the interacting double bond and shortening of the relevant boron-carbon distances related to the central double bond bridge. Another salient feature of the computed structures concerns elongation of the double bond participating in the homoaromatic interaction, as one would intuitively expect. Finally, the most stable forms of all the species considered in Table 2 exhibit *exo*-bending around the central bond, *i.e.* the opposite of that found in the parent *syn*-sesquinorbornene framework.

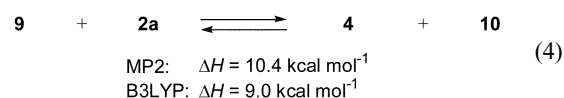
It is also worth noting that the trend of the changes in the optimised geometries on passing from **4** to **5** is close to that found in the related carbocations (Table 1). This is best illustrated by comparison of the computed structures of **4** and **5** with those of **2** and **3**, which in turn reflect the impact of 3-center/2-electron and 4-center/2-electron interactions on the stabilities of these compounds and their geometries. Let us start with structure **4**, and compare the tilting angle  $\alpha$  and the relevant boron-carbon [C(1)–B(11) and C(2)–B(11)] distances of 82.6° and 1.765 Å, respectively, with the corresponding values of the structure **2**. They are 81.6° and 1.718 Å, respectively. We note in passing that these parameters are in fair agreement with the MP2 values of 82.7° and 1.780 Å, respectively, for **12**, as well as with the available X-ray data.<sup>41</sup> It follows that the tilting angles in **2**, **4** and **12** are very close despite a large variation in relevant bond distances. On going from **4** to **5** we observe an increase in the tilting angle  $\alpha$  and the

C(1)–B(11)/C(2)–B(11) distances by 14.1° and 0.209 Å, respectively, which is close to 15.6° and 0.211 Å found between **2** and **3**. A similar trend is encountered for the C(1)–C(2) double bond, which is elongated by 0.017 Å and 0.024 Å, respectively. These changes compare well with the changes observed in the carbocations.

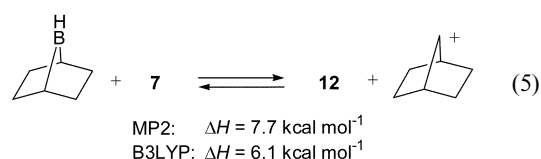
The initial presumption concerning the non-classical nature of boranes **4** and **5** is corroborated by their homoaromatic stabilisation energies, which are estimated by using isodesmic reactions (2) and (3).



It appears that both isodesmic processes are exothermic by –18.3 and –30.9 kcal mol<sup>-1</sup> (–15.2 and –26.5 kcal mol<sup>-1</sup> at the B3LYP level), respectively, indicating that both **4** and **5** are stabilised by interaction of the electron deficient center(s) and the double bond, but to a smaller extent than found in the corresponding cations. This conclusion is reinforced by comparing the stabilisation energies of **4** and **2a** by means of isodesmic equation (4)



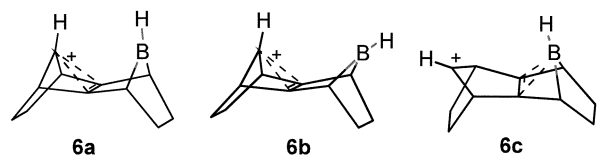
This reaction has an enthalpy change of 10.4 kcal mol<sup>-1</sup> (9.0 kcal mol<sup>-1</sup> at the B3LYP level) implying that homoaromatic interaction in carbocation **2a** is stronger than in borasesquinorbornene **4**. Both findings contradict an earlier proposition by Schulman and Schleyer that homoaromaticity in 7-boranorbornene is more pronounced than in norbornen-7-yl cation.<sup>38</sup> It should be, however, emphasised that the latter result was obtained by employing the MP2/6-31G\*//HF/6-31G\* method. By employing the same approach adopted in the present study we arrived at an enthalpy change for the corresponding reaction (5) of 7.7 kcal mol<sup>-1</sup> (6.1 kcal mol<sup>-1</sup> at the B3LYP level).



This is very close to the previous result obtained by isodesmic reaction (4). It follows that taking explicit account of the electron correlation effects in the determination of geometries of non-classical species is of utmost importance for obtaining reliable energetic data. It is also interesting to note that the homoaromatic SE of **5** is lower than  $2 \times \Delta H$  of eqn. (4), indicating that stabilisation of each of the rings in **5** is smaller than that in **4**.

An interesting model system for pursuing this question further is provided by species **6**, in which <sup>+</sup>CH and BH groups compete for the same double bond. For this ion our calculations predict two energy minima on the MP2, as well as on the B3LYP potential energy surfaces. They are **6a** and **6b** exhibiting comparable energies [–450.34720 au and –450.34699 au (MP2)].

In both systems only the cationic center (<sup>+</sup>CH group) takes part in homoaromatic interaction, as indicated by their geometric parameters (Table 2). It is also worth mentioning that



the orientation of the B–H bond has only a marginal effect on stability of the ion as indicated by the corresponding energies above. We also located structure **6c** with the boron atom oriented toward the central double bond bridge, but this structure was considerably higher in energy (27.5 kcal mol<sup>-1</sup>) and had one imaginary frequency ( $\nu = 415.8i$  cm<sup>-1</sup>) that corresponds to isomerization of the type described earlier for carbocations **2** and **3**.

### <sup>13</sup>C and <sup>11</sup>B NMR chemical shifts and charge distribution

It is well known that <sup>13</sup>C and <sup>11</sup>B chemical shifts are very sensitive to the degree of charge delocalisation. Consequently, they are frequently used for probing the homoaromatic nature of carbocations and boron compounds.<sup>15</sup> In the absence of the experimental NMR data for the species considered in this work we deemed it worthwhile to comment on their computed NMR spectra. The chemical shifts, as mentioned in section 2, were calculated by using the GIAO method at the MP2 and B3LYP geometries. They are listed in Table 4, together with the relevant data for the reference molecules **7** and **12**. Before discussing the general trends of the calculated chemical shifts it is worth noting that use of B3LYP geometry for **7** leads to better agreement with experimental NMR data<sup>42</sup> than calculations employing MP2 geometry. The accuracy of the calculated <sup>11</sup>B chemical shift for **12** is more difficult to assess since the available experimental data<sup>34</sup> refer to the highly substituted derivative of **12** with the phenyl group attached to the boron atom. It is, however, gratifying that the trend of changes in the calculated chemical shifts of the atoms involved in the homoaromatic cycle of the studied species is very similar for both MP2 and B3LYP methods.

The calculated <sup>13</sup>C chemical shifts for the norbornen-7-yl cage in **2a** are very similar to the values calculated for the norbornen-7-yl cation.<sup>34</sup> For example, the  $\delta^{13}\text{C}$  of 28.2 ppm due to the carbocationic center is only 5.7 ppm less deshielded than that of the norbornen-7-yl cation. Similarly, the olefinic carbon atoms in **2a** are predicted to be only slightly (~18 ppm) more deshielded than in the norbornen-7-yl cation. Both results are compatible with conclusion that these two species exhibit similar homoaromatic features. This is also true for the norbornen-7-yl cage in **6a** for which calculations predict  $\delta^{13}\text{C}$  for the cationic center and the olefinic carbon atoms of 33 and 148 ppm, respectively. It is also worth mentioning that all these species exhibit similar charge distribution over the cationic center and olefinic carbon atoms, with the charge at the cationic center (Table 5) within Löwdin's partitioning scheme, being close to zero meaning that the positive charge is strongly delocalized. To be more specific, the notion of the cationic center has the following meaning: it involves a three-coordinated carbon atom, which is slightly more positive than carbons not involved in the homoaromatic cycle. In fact, the positive charge is distributed all over the molecule including in particular the hydrogen atoms. In this regard it is also of interest to compare carbon chemical shifts and charge distribution between **2a** and its "classical" counterpart **2b**. The calculated chemical shift of the charged atom in **2b** is 235.2 ppm, which implies a 206.9 ppm downfield deviation from the  $\delta^{13}\text{C}$  value for that atom in **2a**. The observed trend is in accordance with the pronounced positive charge of this carbon atom in the latter case (Table 5).

Compared to the <sup>13</sup>C chemical shifts of the C(11) atom in **2a** and in **6a**, the chemical shift of the cationic centers in dication **3a** appears to be ~100 ppm downfield. It should be noticed that

cationic centers in **3a** are positively charged in contrast to **2a** where the cationic center is slightly negative (Table 5). This, in turn, suggests that the effectiveness of the charge depletion from the cationic center in the dication is significantly reduced relative to the monocation, in accordance with discussion based on structural arguments.

The calculated <sup>11</sup>B chemical shifts in **4** and **5** are negative, in line with the <sup>11</sup>B chemical shift calculated for 7-boranorbornene (-74.2 ppm), and the experimentally measured value in the Diels–Alder dimer of 1-phenyl-2,3,4,5-tetramethylborole (-14.3 ppm).<sup>32</sup> Apparently, shielding of the boron atom in these species is consistent with the homoaromatic nature of these compounds. The <sup>11</sup>B chemical shift of the 7-boranorbornene ring in **6a** (57.5 ppm), differs substantially from the values calculated for **4** and **5**. It should be pointed out that the <sup>11</sup>B chemical shift in **5** is less shielded than in **4**, suggesting again that homoaromatic interaction within the BCC triangle is stronger in the latter compound. Comparison of the calculated charges for these two species fully supports this conclusion.

## Conclusions

MP2 and DFT calculations at the 6-31G\* level provide interesting insight in the structure and properties of some of the carbocations and their boron analogues embodied in the *syn*-sesquinorbornene framework hitherto not studied experimentally. In particular, it is conclusively shown that they exhibit homoaromatic features on the basis of structural, energetic and magnetic properties evidence. The calculated minimum energy structures of all the species can be understood only by invoking the homoconjugative interaction between the electron deficient center(s) and a carbon–carbon double bond. This is reflected in the characteristic bending of the <sup>+</sup>CH and BH bridges, respectively, toward the central double bond and the lengthening of the latter. Another salient feature of the computed structures concerns the direction of bending of the molecular framework which changes from convex in the parent **1** to concave in non-classical systems.

The use of isodesmic reactions based upon MP2(fc)/6-31G\* energies indicates that homoconjugative stabilisation of mono- and di-cations is greater than those of the corresponding isoelectronic boron compounds. The calculated charge distribution and <sup>13</sup>C and <sup>11</sup>B NMR chemical shifts corroborate this conclusion.

## Acknowledgements

Financial support from the Ministry of Science and Technology of Croatia (Project No. 0098056) is gratefully acknowledged.

## References

- IUPAC name: tetracyclo[6.2.1.1<sup>3,6</sup>0<sup>2,7</sup>]dodec-2(7)-ene.
- Stereochemistry and Reactivity of Systems Containing  $\pi$ -Electrons*, ed. W. H. Watson, VCH International, Deerfield Beach, Florida, 1983.
- (a) K. N. Houk, N. G. Rondan, F. K. Brown, W. L. Jorgensen, J. D. Madura and D. C. Spellmeyer, *J. Am. Chem. Soc.*, 1983, **105**, 5980; (b) P. H. Mazzocchi, B. Stahly, J. Dodd, N. G. Rondan, L. N. Domelsmith, M. D. Rozeboom, P. Caramella and K. N. Houk, *J. Am. Chem. Soc.*, 1980, **102**, 6482; (c) N. G. Rondan, M. N. Paddon-Row, P. Caramella and K. N. Houk, *J. Am. Chem. Soc.*, 1981, **103**, 2436; (d) N. G. Rondan, M. N. Paddon-Row, P. Caramella, J. Mareda, P. H. Mueller and K. N. Houk, *J. Am. Chem. Soc.*, 1982, **104**, 4974.
- (a) R. Gleiter and J. Spanget-Larsen, *Tetrahedron Lett.*, 1982, **23**, 927; (b) J. Spanget-Larsen and R. Gleiter, *Tetrahedron*, 1983, **39**, 3345.
- P. D. Bartlett, A. J. Blakeney, M. Kimura and W. H. Watson, *J. Am. Chem. Soc.*, 1980, **102**, 1383.

- 6 (a) W. H. Watson, J. Galloy, P. D. Bartlett and A. A. M. Roof, *J. Am. Chem. Soc.*, 1981, **103**, 2022; (b) O. Ermer, *Tetrahedron*, 1974, **30**, 3103; (c) J.-P. Hagenbuch, P. Vogel, A. A. Pinkerton and D. Schwarzenbach, *Helv. Chim. Acta*, 1981, **64**, 1818; (d) L. A. Paquette, T. M. Kravetz and L.-Y. Hsu, *J. Am. Chem. Soc.*, 1985, **107**, 6598.
- 7 In this paper the out-of-plane deformation of a double bond will be described using the flap or hinge angle  $\phi: 180^\circ - \gamma$ , where  $\gamma$  corresponds to dihedral angle between C(3)–C(2)–C(1)–C(4) and C(6)–C(2)–C(1)–C(5) planes. For alternative descriptions of the pyramidalization angles see references 9,10 and 11.
- 8 O. Ermer and C.-D. Bodecker, *Helv. Chim. Acta*, 1983, **66**, 943.
- 9 W. T. Borden, *Chem. Rev.*, 1989, **89**, 1095.
- 10 S. F. Nelsen, T. B. Frigo and Y. Kim, *J. Am. Chem. Soc.*, 1989, **111**, 5387.
- 11 R. C. Haddon, *J. Am. Chem. Soc.*, 1990, **112**, 3385.
- 12 I. Antol, M. Eckert-Maksić, D. Margetić, Z. B. Maksić, K. Kowski and P. Rademacher, *Eur. J. Org. Chem.*, 1998, 1403.
- 13 D. Margetić, R. N. Warrenner, M. Eckert-Maksić, I. Antol and Z. Glasovac, *Theor. Chem. Acc.*, in press.
- 14 M. Eckert-Maksić, *Photoelectron Spectroscopy of Alcohols, Phenols, Ethers and Peroxides in: Chemistry of Hydroxyl, Ether and Peroxide Groups*, ed. S. Patai, J. Wiley, Chichester, Suppl. E2, 1993, pp. 299–371.
- 15 For a recent review article see e.g. R. V. Williams, *Chem. Rev.*, 2001, **101**, 1185.
- 16 P. C. Hariharan and J. A. Pople, *Theor. Chim. Acta*, 1973, **28**, 213.
- 17 (a) A. D. Becke, *J. Chem. Phys.*, 1993, **98**, 5648; (b) C. Lee, W. Yang and R. G. Parr, *Phys. Rev. B*, 1988, **37**, 785; (c) B. Michlich, A. Savin, H. Stoll and H. Preuss, *Chem. Phys. Lett.*, 1989, **157**, 200; (d) P. J. Stephens, F. J. Devlin, C. F. Chabalowski and M. J. Frisch, *J. Phys. Chem.*, 1994, **98**, 11623.
- 18 (a) J. A. Pople, J. S. Binkley and R. Seeger, *Int. J. Quantum Chem. Symp.*, 1976, **10**, 1; (b) R. Krishnan and J. A. Pople, *Int. J. Quantum Chem.*, 1978, **14**, 91.
- 19 A. P. Scott and L. Radom, *J. Phys. Chem.*, 1996, **100**, 16502.
- 20 C. Gonzalez and H. B. Schlegel, *J. Phys. Chem.*, 1990, **94**, 5523.
- 21 (a) K. Wolinski, J. F. Hinton and P. Pulay, *J. Am. Chem. Soc.*, 1990, **112**, 8251; (b) R. Ditchfield, *Mol. Phys.*, 1974, **27**, 789.
- 22 P.-O. Löwdin, *J. Chem. Phys.*, 1950, **18**, 365.
- 23 C. M. Breneman and K. B. Wiberg, *J. Comput. Chem.*, 1990, **11**, 361.
- 24 K. Jug and Z. B. Maksić, in *Theoretical Models of Chemical Bonding*, ed. Z. B. Maksić, vol. 3., *Molecular Spectroscopy, Electronic Structure and Intramolecular Interactions*, Springer Verlag, Berlin–Heidelberg, 1991, pp. 235–288.
- 25 Z. B. Maksić, in *Theoretical Models of Chemical Bonding*, ed. Z. B. Maksić, vol. 3., *Molecular Spectroscopy, Electronic Structure and Intramolecular Interactions*, Springer Verlag, Berlin–Heidelberg, 1991, pp. 289–340.
- 26 GAUSSIAN 94, Revision B.3 M. J. Frisch, G. W. Trucks, H. B. Schlegel, P. M. W. Gill, B. G. Johnson, M. A. Robb, J. R. Cheeseman, T. Keith, G. A. Peterson, J. A. Montgomery, K. Raghavachari, M. A. Al-Lahan, V. G. Zakrzewski, J. L. Andreas, E. S. Replogle, R. Gomperts, R. L. Martin, D. J. Fox, J. S. Binkley, D. J. Defrees, J. Baker, J. P. Stewart, M. Head-Gordon, C. Gonzales and J. A. Pople, Gaussian Inc., Pittsburg PA, 1995.
- 27 GAMESS M. W. Schmidt, K. K. Baldridge, J. A. Boatz, S. T. Elbert, M. S. Gordon, J. H. Jensen, S. Koseki, N. Matsunaga, K. A. Nguyen, S. J. Su, T. L. Windus, M. Dupuis and J. A. Montgomery, *J. Comput. Chem.*, 1993, **14**, 1347.
- 28 (a) M. C. Holthausen and W. Koch, *J. Phys. Chem.*, 1993, **97**, 10021; (b) R. V. Williams, W. D. Edwards, V. R. Gadgil, M. E. Colvin, E. T. Seidl, D. v. der Helm and M. B. Hossain, *J. Org. Chem.*, 1998, **63**, 5268; (c) A. G. Griesbeck, T. Deufel, G. Hohlneicher, R. Rebentisch and J. Steinwascher, *Eur. J. Org. Chem.*, 1998, 1759.
- 29 See e.g. W. J. Hehre, L. Radom, P. v. R. Schleyer and J. A. Pople, *Ab Initio Molecular Orbital Theory*, Wiley, New York, 1986.
- 30 W. Koch and M. C. Holthausen, *A Chemist's Guide to Density Functional Theory*, Wiley-VCH, Weinheim, 1999.
- 31 (a) S. Winstein and C. Ordroneau, *J. Am. Chem. Soc.*, 1960, **82**, 2084; (b) H. C. Brown, *Acc. Chem. Res.*, 1973, **6**, 377; (c) P. R. Story and B. C. Clark, in *Carbonium Ions*, eds. G. A. Olah and P. v. R. Schleyer, Wiley, New York, 1972, ch. 23; (d) H. C. Brown, *The Nonclassical Ion Problem*, Plenum Press, New York, 1977; (e) M. Saunders and Jimenez-Vazquez, *Chem Rev.*, 1991, **91**, 375.
- 32 (a) S. Winstein, M. Shatavsky, C. Norton and R. B. Woodward, *J. Am. Chem. Soc.*, 1955, **77**, 4183; (b) S. Winstein and E. T. Stafford, *J. Am. Chem. Soc.*, 1957, **79**, 505; (c) W. G. Woods, R. A. Carboni and J. D. Roberts, *J. Am. Chem. Soc.*, 1956, **78**, 5653.
- 33 (a) P. R. Story and M. Saunders, *J. Am. Chem. Soc.*, 1962, **84**, 4876; (b) G. A. Olah and A. M. White, *J. Am. Chem. Soc.*, 1969, **91**, 3954.
- 34 M. Bremer, K. Schötz, P. v. R. Schleyer, U. Fleischer, M. Schindler, W. Kutzelnigg, W. Koch and P. Pulay, *Angew. Chem., Int. Ed. Engl.*, 1989, **28**, 1042.
- 35 (a) T. Laube, *J. Am. Chem. Soc.*, 1989, **111**, 9224; (b) J. W. Evans, K. J. Forrester and J. W. Ziller, *J. Am. Chem. Soc.*, 1995, **117**, 12635.
- 36 1 kcal mol<sup>-1</sup> = 4.184 kJ mol<sup>-1</sup>.
- 37 Present work, see also ref. 34.
- 38 J. M. Schulman, R. L. Disch, P. v. R. Schleyer, M. Bühl, M. Bremer and W. Koch, *J. Am. Chem. Soc.*, 1992, **114**, 7897.
- 39 An independent synchronous transition-guided quasi-Newton (QST2) calculation<sup>40</sup> for isomerization of **3d** into **3d'** also resulted in **3c** as the transition structure.
- 40 C. Peng, P. Y. Ayala, H. B. Schlegel and M. J. Frisch, *J. Comput. Chem.*, 1996, **17**, 49.
- 41 (a) P. J. Fagan, E. G. Burns and J. C. Calabrese, *J. Am. Chem. Soc.*, 1988, **110**, 2979; (b) P. J. Fagan, W. A. Nugent and J. C. Calabrese, *J. Am. Chem. Soc.*, 1994, **116**, 1880.
- 42 G. A. Olah, G. Liang, G. D. Mateesen and J. L. Riemenschneider, *J. Am. Chem. Soc.*, 1975, **97**, 6803.